buildings

MDPI

Article

Evaluation of the Nonlinear Seismic Responses of High-Rise Reinforced Concrete Buildings with Different Foundations and Structural Plans—Considering Soil-Structure Interactions

Talha Polat Doğan [1] and Ibrahim Hakkı Erkan [2,*]

[1] Faculty of Engineering, Gazi University, 06570 Ankara, Türkiye; polatdogan@gazi.edu.tr
[2] Faculty of Engineering and Natural Sciences, Konya Technical University, 42000 Konya, Türkiye
* Correspondence: iherkan@ktun.edu.tr

Abstract: Regarding the behavior of reinforced concrete structures under seismic loads, the interaction between structure and soil is as important as the load-bearing system and foundation type. This study was designed to assess the effect of structural types and soil–structure interactions (SSIs) on the responses of reinforced concrete (RC) buildings to earthquakes. Therefore, nonlinear time history analyses were performed on 20-storey RC buildings. In this analysis, three different structural system types and three different foundation types were considered for the parametric study. The numerical results obtained from the nonlinear dynamic analysis were criticized in terms of base shear force and roof displacement. Based on the obtained numerical results, utilizing SSI in the nonlinear time history analysis of the RC buildings improved the overall structural integrity by delaying plastic hinge formation and preventing the total failure of structural elements. Base shear forces increased up to 20% for the same structural system and different SSI situations, and up to 60% for different structural systems and the same SSI situation. Roof displacements increased up to 17% for the same structural system and different SSI situations, and up to 24% for different structural systems and the same SSI situation. All of the behavioral differences showed the importance of considering the SSI in the design stage of the buildings.

Keywords: soil–structure interaction; earthquake-resistant design; tall buildings; earthquake behavior; soil springs

check for updates

Citation: Doğan, T.P.; Erkan, I.H. Evaluation of the Nonlinear Seismic Responses of High-Rise Reinforced Concrete Buildings with Different Foundations and Structural Plans—Considering Soil-Structure Interactions. *Buildings* **2024**, *14*, 1686. https://doi.org/10.3390/buildings14061686

Academic Editor: Andreas Lampropoulos

Received: 27 April 2024
Revised: 29 May 2024
Accepted: 3 June 2024
Published: 6 June 2024

Copyright: © 2024 by the authors. Licensee MDPI, Basel, Switzerland. This article is an open access article distributed under the terms and conditions of the Creative Commons Attribution (CC BY) license (https://creativecommons.org/licenses/by/4.0/).

1. Introduction

In contemporary urban areas, the seismic performance of structures is directly linked to their resilience against earthquake effects. The design and construction of buildings are critically important for the safety of millions of people residing in earthquake-prone regions. However, traditional approaches in structural engineering often utilize simplified models when considering the interaction between buildings and soil. In reality, the interaction between buildings and soil is highly complex, and the effects of this interaction significantly determine seismic performance [1–3].

To comprehend and consider for this complexity, research focusing on the relationship between buildings and soil–structure interactions (SSIs) has gained importance. The study of SSI aims at investigating the interaction between buildings and the ground to more accurately predict the seismic behavior of structures. In this context, a complex system emerges where factors such as the fundamental properties of structures, soil characteristics, and earthquake effects converge [4–7].

Particularly, devastating natural disasters like the 6th of February Kahramanmaraş earthquake have further underscored the significance of soil–structure interactions. This earthquake, which occurred in the city of Kahramanmaraş in southern Turkey, resulted in severe damage [8,9]. The impact of the earthquake once again emphasized the importance of SSI factors that need to be considered in the design and construction of buildings.

This article aims to examine the soil–structure interaction of buildings and evaluate the effects of this parameter on seismic performance. Recent developments in the relevant literature highlight the importance of SSI in the structural design and earthquake engineering fields, and present significant findings that will shed light on future research. Analyses of the February 6th Kahramanmaraş earthquakes have shown that one of the main causes of the loss of life and destruction was the weak soil in the region. Especially in Hatay, Kahramanmaraş, and Adıyaman, where weak soils (C and D, as given in Eurocode8 [10]) are commonly found, this resulted in significant losses [8]. In the referenced study, the recorded earthquake accelerations in the Hatay region indicated that the high death toll and destruction were due to the thick layers of loose alluvial soil and the proximity of groundwater to the surface. Therefore, the results obtained from this study demonstrate the necessity of making soil–structure interaction (SSI) a mandatory component when simulating the actual behavior of structures built on loose alluvial soils in seismically active regions. Since TBEC2018 does not mandate the application of SSI for buildings below 105 m, this study was conducted to emphasize the importance of this requirement.

Many studies have been performed and applications investigated to observe the behavior of structures during earthquakes and to determine the seismic performance of structures, but without considering soil effects [4,11–14]. This may lead to two different situations in a building, especially during an earthquake. In the first of these situations, deformations in the soil may cause the formation of different modal shapes in the building, resulting in the structure exhibiting unexpected behaviour, which may even lead to the building resonating. Inferences from recent seismic activities suggest that fixed-base assumptions could be misleading, and neglecting the influence of soil effects could cause unsafe design, particularly for structures founded on soft soils. Another consequence of not considering soil effects is the emergence of overdesigned buildings with compromised safety conditions [5,8,15–17].

During an earthquake, the lateral loads caused by the effect of inertia are transferred to the soil underneath the building with the foundation elements and these elements are in connection with other structural system elements. High-fidelity results have been proven in recent studies examining structure–soil interactions with analytical and experimental studies [5,7]. In studies examining the behavior of structures against seismic loads, the soil–structure connection points are generally accepted as fully rigid (fixed base), and the effect of the soil on the structure behavior is neglected. However, under the influence of both static and dynamic loads, the structure moves with the ground and the foundation systems can be located in different positions on the ground, especially during dynamic loading [4,6,18–20]. For this reason, analyses made by ignoring the SSI are open to discussion and may lead to negative results.

The energy-consuming mechanisms in foundation–ground systems always reduce the seismic demand of a structure compared to fixed-base designs. On the other hand, an increase in the overall structural system deformation can reduce (damping) or increase (resonance) the inertial forces on the structure depending on the frequency of the earthquake record [18,21]. Considering the seismic behavior of high-rise buildings, rotations in the foundations play an important role in the lengthening of the fundamental period [22–24]. The formation of plastic mechanisms in the soil–foundation system can lead to the partial isolation of the superstructure against seismic effects [25,26]. Research has shown that seismic motion in foundations generally increases lateral displacement, not including seismic isolation, which is of minor importance in the seismic performance of slender structures [27–29]. However, a more general conclusion has been presented that the effect of foundation rocking on structural deformation is mainly dependent on the value of the fundamental period of the building in the elastic spectrum of the earthquake record [14,29,30].

Contrary to the fixed-base assumption, which is based on the principle of limiting drifts and rotations on the basis of the superstructure, the SSI is the consideration that foundation elements can be deformed according to the mechanical properties of the soil. The differences

in the behaviors of structures in line with the SSI and the fixed-base assumption are shown in Figure 1 [5]. Here, while only displacements due to the lateral displacement capacity of the structure can be mentioned for the fixed-base assumption, with the SSI, it is also possible to discuss additional displacements resulting from movements such as rotation and displacement at the foundation, in addition to structural lateral displacement rigidity.

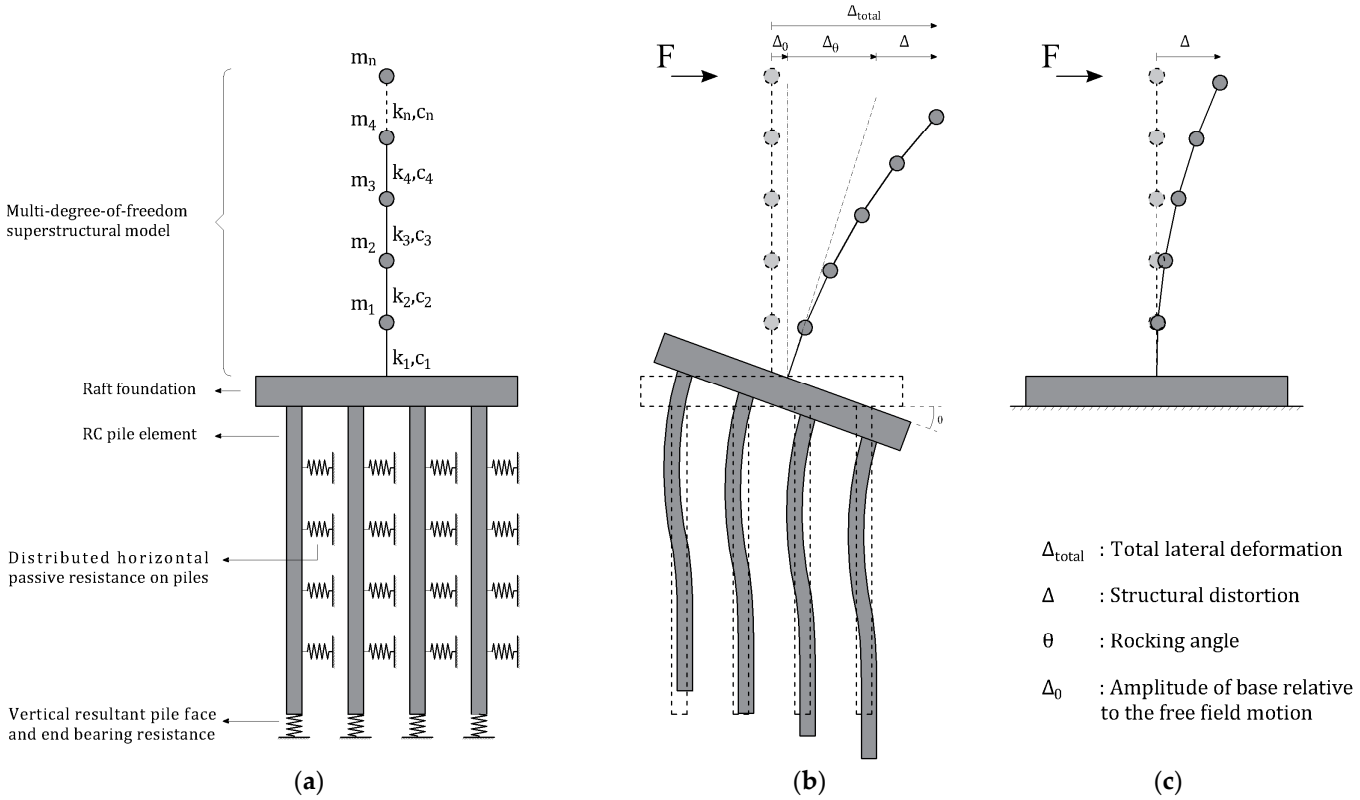


Figure 1. The difference in the behavior of structures considering SSI and fixed-base assumption. (**a**) Piled raft-supported structure and foundation springs, (**b**) lateral deformation of the SSI structure due to rocking motion, (**c**) lateral deformation of the fixed-base structure [5].

Compared to current studies in the literature, which mostly focus on the behavior of low- and mid-rise buildings in relation to the SSI, this study aims to observe the responses of high-rise buildings that are designed with different structural systems. As is known, high-rise buildings have longer fundamental periods, which reduces base shear, but considering the SSI, increases roof displacement. This study was prepared to observe the behavioral differences between multi-storey residential buildings in relation to the SSI. RC building models were examined by combining fixed support, raft foundations, and piled–raft foundations separately for each structural system type. The aim here was to investigate the behavioral differences between the three structural systems coupled with three different SSI conditions under an input earthquake. Different soil types were not included in the parametric study.

Instead of obtaining structure performance as a result of nonlinear time history analyses, the main purpose of this study was to investigate the effects of soil–structure interactions on structural behavior under seismic effects. Therefore, the analyses performed were applied in only one direction to analysis models with symmetrically designed structural systems.

2. Modelling of RC Buildings and SSI

2.1. Structural Systems Designed for Analysis Models

Three 20-storey building models, designed following the regulations given in TBEC2018 [31], were coupled with three different SSI conditions. The models had a

32 × 32 m^2 plan area and a total height of 60 m above ground. As presented in Figure 2, the floor plans were symmetrical in both the X and Y directions for each structural system. The main differences that distinguished the structural systems from each other were the response modification factors given in TBEC2018, which depend on the shear wall ratio. The RC shear wall ratio specified in TBEC 2018 is defined as follows: *the ratio of the total cross-sectional areas belonging to the RC shear walls in any selected direction on the storey that will be affected by the largest amount of seismic load, to the total of all the plan areas of the building. Structural systems of buildings are accepted as SWs when this ratio meets the following conditions (Equations (1) and (2))*. For buildings with SWs, the response modification factor is specified as R = 6 in TBEC 2018 [31].

$$\sum A_g / \sum A_p \geq 0.002 \quad (1)$$

$$V_t / \sum A_g \leq 0.5 f_{ctd} \quad (2)$$

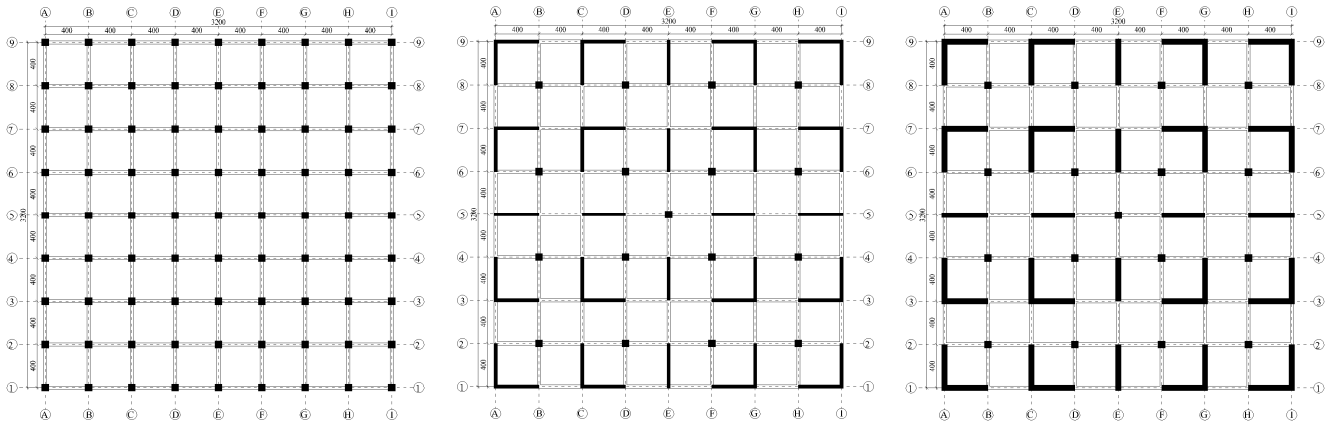


Figure 2. Structural systems of the analysis models designed. (**a**) Model 1; (**b**) Model 2; (**c**) Model 3.

In these inequalities, A_g represents the total RC shear wall cross-sectional area, A_p represents the plan area of one floor, and V_t represents the base shear force affecting the building. As can be understood from the given conditions, if the RC shear wall ratio value is less than 0.002, the structural system of the building consists of moment frames with RC shear walls (MF-SWs). For buildings like this, the response modification factor is R = 7. If the building does not have an RC shear wall, the structural system of the building consists of moment frames (MFs). For buildings like this, the response modification factor is R = 8. These R factors given in TBEC 2018 are for the structures that are designed following the principle of high ductility [31]. Considering the RC shear wall ratio, the first model (shear wall ratio: 0‰) consists of MFs, the second model (shear wall ratio: 1‰) consists of MF-SWs, and the third model (shear wall ratio: 2‰) consists of SWs, as given in Table 1.

Table 1. The nomenclature of analysis models according to structural systems.

Structural System Type	Model Name
Moment Frames (MFs)/Fixed Base	Model 1.A
Moment Frames (MFs)/Raft	Model 1.B
Moment Frames (MFs)/Piled Raft	Model 1.C
Moment Frames with Shear Walls (MF − SW)/Fixed Base	Model 2.A
Moment Frames with Shear Walls (MF − SW)/Raft	Model 2.B
Moment Frames with Shear Walls (MF − SW)/Piled Raft	Model 2.C
Shear Walls (SW)/Fixed Base	Model 3.A
Shear Walls (SW)/Raft	Model 3.B
Shear Walls (SW)/Piled Raft	Model 3.C

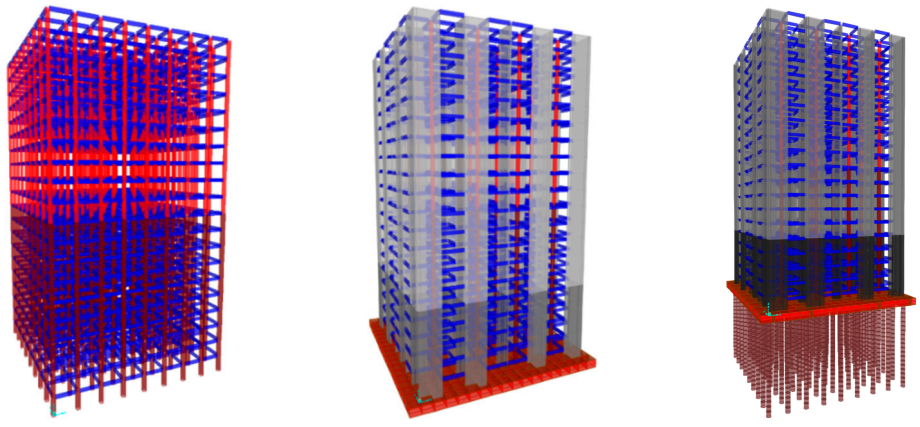
Here, it is seen that the floor plans of Model 2 and Model 3 are similar and the locations of the elements in these plans are kept constant. This was intentional during the design of the structural systems because differences in the distribution of RC walls in the floor plans would prevent a fair comparison of the analysis results at the end of the study. However, the RC shear wall thickness used in Model 2 was doubled in Model 3 to provide RC shear wall ratio values that could determine structural system differences.

Sap2000 was used in the conducted analyses as it allows for the detailed design of structural elements and has frequently been preferred in recent studies in the literature [32]. The structural system elements were designed under Mander's Confined Concrete Theory, which is a built-in option in Sap2000 [33]. This option allows the user to obtain moment–rotation and P-M-M diagrams to determine the plastic hinge properties of the structural elements. The section properties given in Table 2 were determined under the design loads given in ASCE7-10 and TS498 [34,35], and lateral design loads were obtained using response spectrum analysis [36]. All structural elements were designed according to the *Load and Resistance Factor* (LRFD) design method. In Figure 3, coupled analysis models and foundation types are given to represent one of each structural system and foundation type. Plastic hinges, one of the requirements for nonlinear analyses, were defined in accordance with the provisions in TBEC2018 and ASCE41-13. The plastic rotation limits for the plastic hinges are presented in Table 3 [31,37].

Table 2. Cross-sectional properties of structural system elements.

Element Type	Rebar Type		Rebar Magnitude	Confinement Rebar
Column 65 × 65 cm (H < 30 m)	Longitudinal		8 ϕ 16	ϕ 8/10
Column 55 × 55 cm (H > 30 m)	Longitudinal		8 ϕ 16	ϕ 8/10
Beam 30 × 60 cm	Bottom Top		4 ϕ 12 5 ϕ 12	ϕ 8/10
Shear Wall 400 × 50 cm (Model 3)	F: 100 cm W: 200 cm	HCR	2 × 26 ϕ 16 + 18 ϕ 16	ϕ 8/10
	F: 50 cm W: 300 cm	H > HCR	2 × 16 ϕ 16 + 28 ϕ 16	
Shear Wall 400 × 25 cm (Model2)	F: 100 cm W: 200 cm	HCR	2 × 22 ϕ 16 + 18 ϕ 16	ϕ 8/10
	F: 50 cm W: 300 cm	H > HCR	2 × 16 ϕ 16 + 28 ϕ 16	
Piles D100 cm	Longitudinal		40 ϕ 16	ϕ 8/15

F: flange of RC shear walls; W: web of RC shear walls; HCR: critical height of shear walls.



(**a**) (**b**) (**c**)

Figure 3. Sap2000 models of buildings analyzed. (**a**) MRFs with fixed support; (**b**) SW-MRFs with raft foundation; (**c**) SWs with piled raft foundation.

Table 3. Plastic rotation limits given in TBEC2018.

Damage Level	Plastic Rotation Limit (θ_p)
Collapse Prevention (CP)	$\theta_p^{(CP)} = \frac{2}{3}\left((\Phi_u - \Phi_y) L_p \left(1 - 0.5\frac{L_p}{L_s}\right) + 4.5\,\Phi_u\, d_b\right)$
Life Safety (LS)	$\theta_p^{(LS)} = 0.75\,\theta_p^{(CP)}$
Immediate Occupancy (IO)	$\theta_p^{(SH)} = 0$

θ_p: plastic rotation; Φ_u: ultimate curvature; Φ_y: yielding curvature; L_p: plastic hinge length; L_s: shear bay width; d_b: longitudinal rebar diameter.

2.2. Design of Foundations Determined for Analysis Models

To observe the effect of the SSI, we aimed to determine the soil properties of the modelled buildings and to design different foundations on this soil. In the literature, researchers have determined some parameters to model soil in nonlinear analysis with SSI, such as soil density, shear wave velocity, and Poisson's ratio. Other strength and stiffness parameters (cohesion, bulk modulus, internal friction angle) related to soil that should be used in the analysis are determined via calculations from these values with various correlations and relations [38–40]. With these data, analyses can be performed by defining the ground as a spring element in programs that perform finite element analysis [41,42].

In the regions affected by the Kahramanmaraş earthquake, areas where destruction was observed typically had weak soil conditions. Therefore, in this study, a weak soil type was chosen. Additionally, since considering the soil–structure interaction is not mandatory in TBEC2018 except for in the study of special structures, weak soil with low bearing capacity was used to observe the structural behavior of the buildings and emphasize the importance of considering soil–structure interactions. Consequently, different types of soils were not included in the parametric studies.

The soil used in the analyses was modelled using the Mohr–Coulomb model, which is also known as the elastic–perfectly plastic model. The type of soil addressed in this study, which has a relatively low bearing capacity, was adopted as a single layer with an average standard penetration value of N_{60} = 5–7, average shear wave velocity of V_s = 150 m/s, friction angle of ϕ = 20, and average undrained shear strength (c_u) of 70 KPa. This soil, taking into consideration the soil–structure interaction (SSI), has been determined as ZE (class D for Eurocode8 [10]) according to the soil classification specified in TBEC 2018 [31]. These soils are defined as follows: deposits of loose-to-medium cohesionless soils (with or without some soft cohesive layers) or predominantly soft-to-firm cohesive soils.

The models that were analyzed without consideration of the soil–structure interaction were fixed to the ground with fixed supports at 0 elevation. However, building models designed with the soil–structure interaction in mind were combined with two different foundation types. The first one was the raft foundation with a thickness of 1.5 m. The second foundation type was a 1.5 m thick raft foundation sitting on 81 piles with a depth of 20 m and a diameter of 1 m.

The subgrade module value (k_0) of the clay soil, determined according to the soil class, was accepted as 20,000 kN/m^2/m as a result of calculations and consultations [16,41,43]. The lateral subgrade module value of the soil was calculated as well to prevent lateral displacement. The same subgrade module value was used when defining the area spring on the raft foundation designed with the shell finite element model.

Most soil models that represent soil behavior have a nonlinear, hyperbolic stress–strain relationship. Using nonlinear stress–strain relations that can adequately represent the behavior of both soil and building foundation systems, the main objective of SSI analysis is to accurately determine the soil effects that will occur on the bearing systems of structures [5]. In addition, while 2D models are frequently encountered in the analyses carried out in the literature on this subject [44–46], it has been noted that the results obtained from studies in which 3D models were used in the analyses gave more realistic results [5,47–50]. The calculations of the spring coefficients of the soil springs are modelled as the determinants of displacements that may occur laterally in the pile group. The soil

model, which was adapted to pile groups by Terzaghi and proposed by Winkler in 1867, represents the modelling of soil with spring elements [42,51]. There are two important points to be considered in defining the properties of these springs: first is that the value of spring stiffness varies depending on the depth in the soil, and second is that the stiffness of a spring, which changes with depth, can also change with the displacement of a pile. Considering this situation, the lateral spring coefficients that vary depending on the depth calculated using the subgrade module value are given in Figure 4. In this approach, soil behavior is simulated using a series of vertical nonlinear springs that respond to settlement and rocking movements. The stiffness values are calculated using equations provided by Gazetas [52]. The values of lateral spring coefficients can be found using Equation (3) [19].

$$k_y = k_0 \, z^{1/2} \quad (3)$$

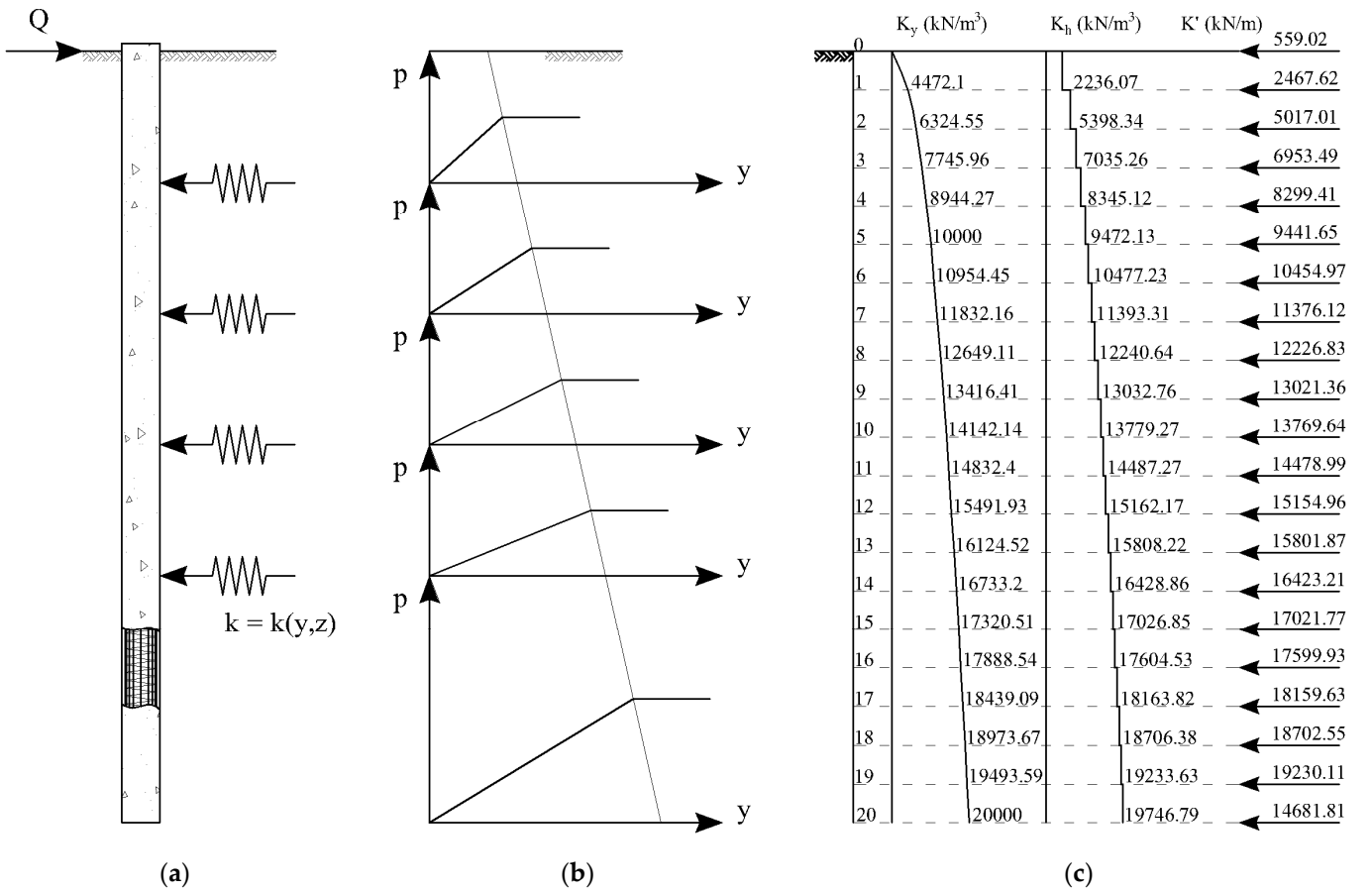


Figure 4. Lateral pile spring strengths. (**a**) Winkler spring model implementation scheme; (**b**) depth-dependent spring stiffness variation scheme; (**c**) determined horizontal spring stiffnesses depending on depth [19].

Regarding the symbols specified in this formula, k_y is the lateral subgrade module that changes in relation to the depth of the soil, k_0 is the subgrade module of the soil, and z is the ratio of the distance to the top of the pile and the length of the pile (L'/L). Since the k_y values given in Figure 4 show a parabolic increase, these values are linearly interpolated and a simplified distribution of the values in the k_h column is obtained. Finally, using the area value determined for each spring element, the k' values, which are the spring coefficient values, can be calculated.

Here, the horizontal spring stiffness values obtained were assigned to the pile elements as nonlinear springs. The vertical springs, representing the pile's lateral friction and tip effects, were also defined as nonlinear springs for the spring node and raft shell elements.

3. Nonlinear Time History Analysis

TBEC2018 divides the spectral definitions to be used in the design of buildings into four different levels. These are defined as "*Seismic Levels*" (DD#) in Table 4. Unless classified as high-rise buildings, residential-type structures are required to be designed according to DD2 in TBEC2018 [53].

Table 4. Seismic levels defined in TBEC2018.

Seismic Levels (DD#)	The Probability of Exceedance in 50 Years	Return Period (Years)
DD1	2%	2475
DD2	10%	475
DD3	50%	72
DD4	68%	43

The Pazarcık earthquake that occurred in Turkey on 6 February 2023 was a seismic event with a magnitude of MW7.7, covering an affected area of 10 provinces. The acceleration spectrum and input record obtained from station DEMP-3126 for this earthquake are shown in Figure 5 [53,54]. In Figure 5a, the design spectra corresponding to the seismic levels in TBEC2018 are compared with the spectrum of the Pazarcık earthquake, and the periods of the building models included in this study are marked on the earthquake spectrum. As seen, the accelerations in the spectral range corresponding to the building periods not only exceed the design spectrum of DD2, but also exceed the values of the DD1 spectrum. The acceleration record corresponding to the earthquake is compared with the scaled DD2 spectrum in Figure 5b. It was evident that such a strong ground motion would serve as a good test for the building models designed within the scope of the study. Therefore, the existing models were subjected to time history analyses without scaling the acceleration records, assuming that they were at the location of station 3126, which had similar soil properties to the selected site class in the study where the acceleration records were obtained [3,30,31,55]. Although the floor plans of the building models are symmetric in both directions, the vectorial seismic components of the earthquake in the N-S and E-W directions were applied simultaneously to the building models. In the results section, the results from the N-S direction, which are larger and more critical, are analyzed.

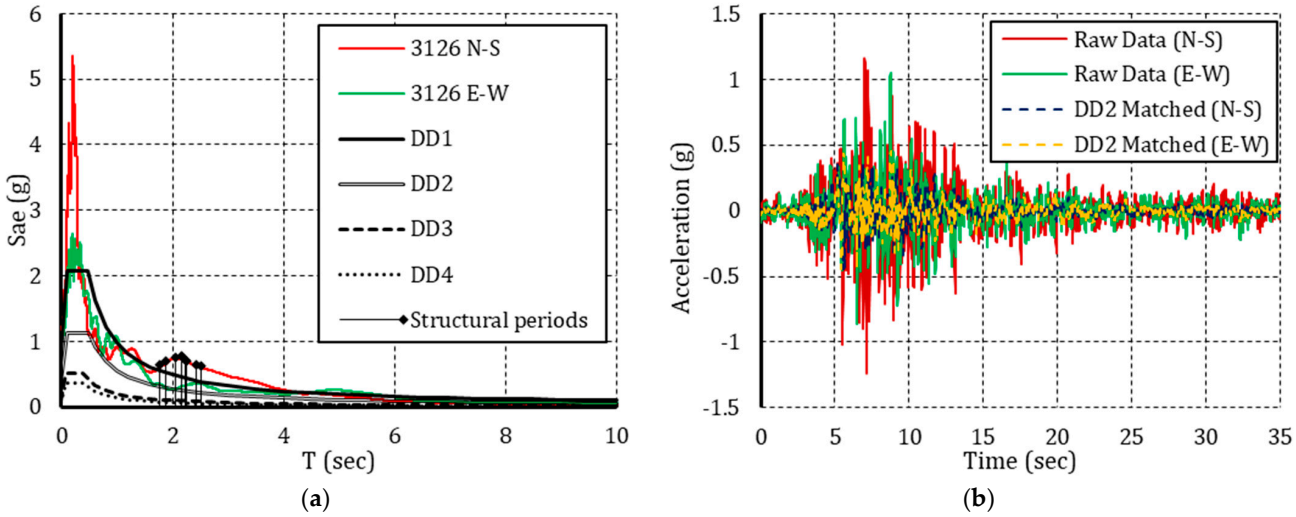


Figure 5. (**a**) Elastic response spectra; (**b**) acceleration record of the input earthquake and scaled input [53].

4. Analysis Results

4.1. Results of Nonlinear Time History Analysis

After the nonlinear time history analyses were performed, the numerical data obtained from Sap2000 [32] were gathered and presented as charts to compare different building

models in terms of earthquake behavior. Figures 6 and 7 show the base shear forces obtained from the nonlinear analysis. Figures 8 and 9 show the ratio of roof displacement to total building height. The investigations into base shear and roof displacement were interpreted by comparing the absolute maximum values.

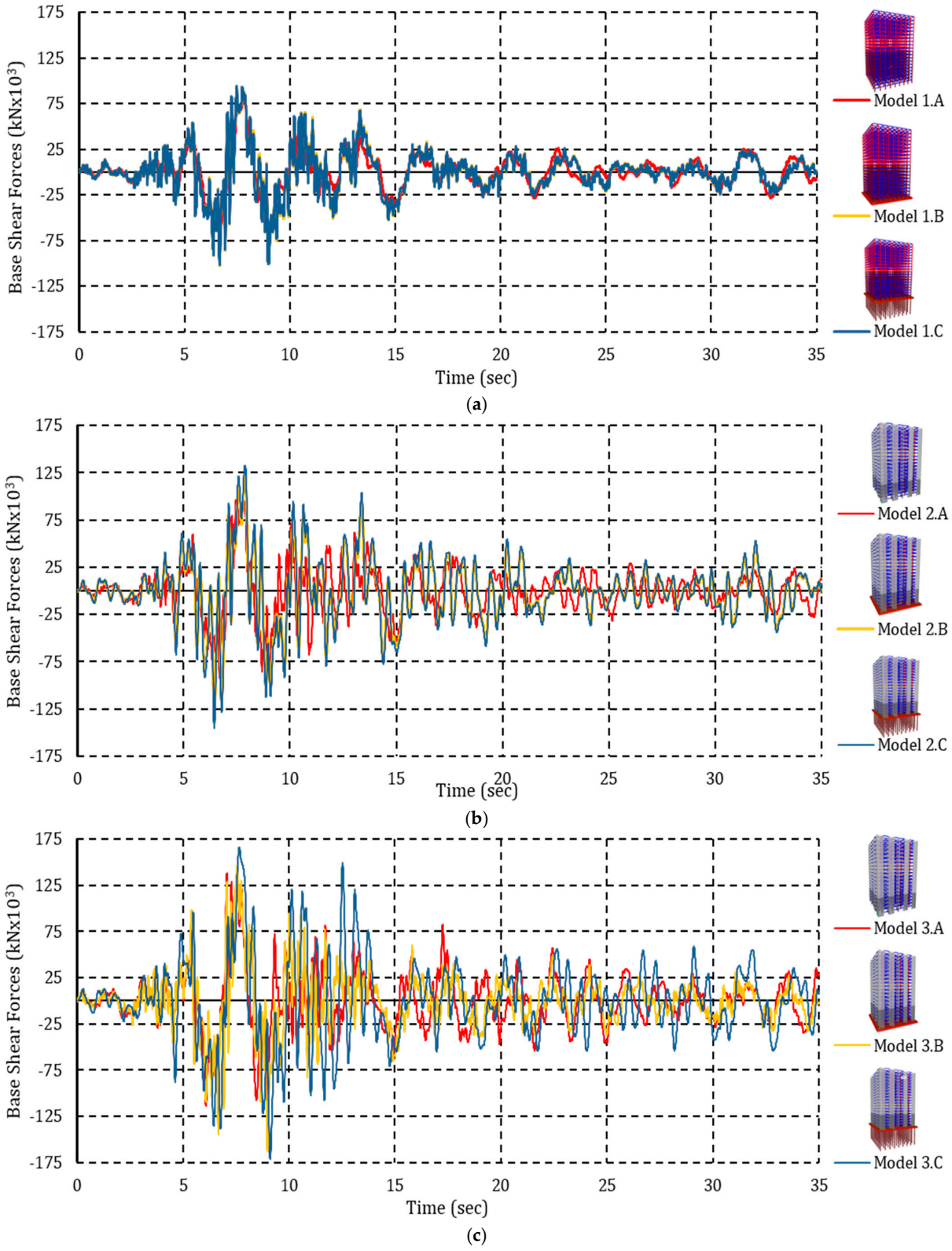


Figure 6. Base shear force for the models with the same structural system. (**a**) Different SSI for MFs; (**b**) different SSI for SW-MFs; (**c**) different SSI for SWs.

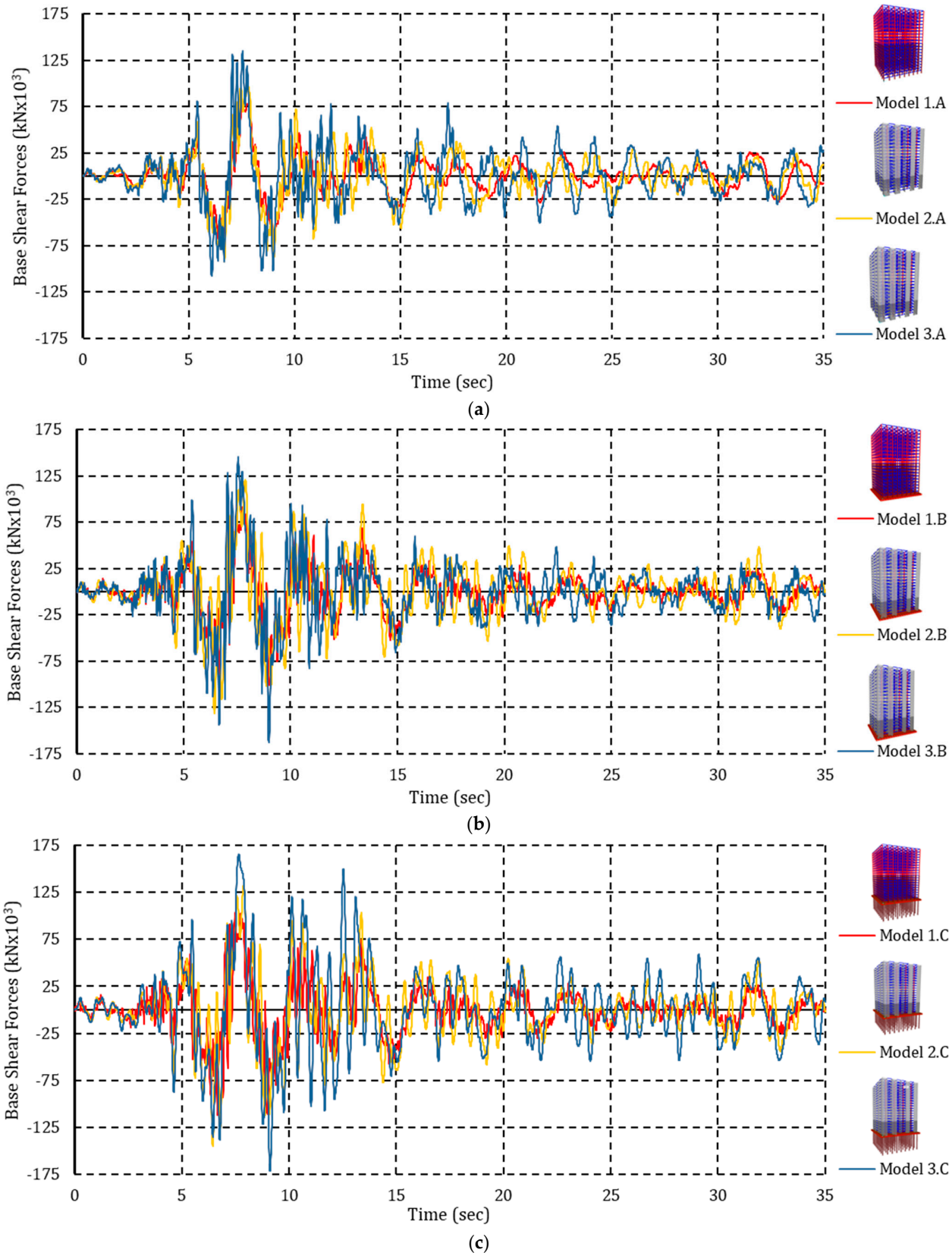


Figure 7. Base shear force for the models with the same SSI condition. (**a**) Different structural systems with fixed support; (**b**) different structural systems with raft foundation; (**c**) different structural systems with piled raft foundation.

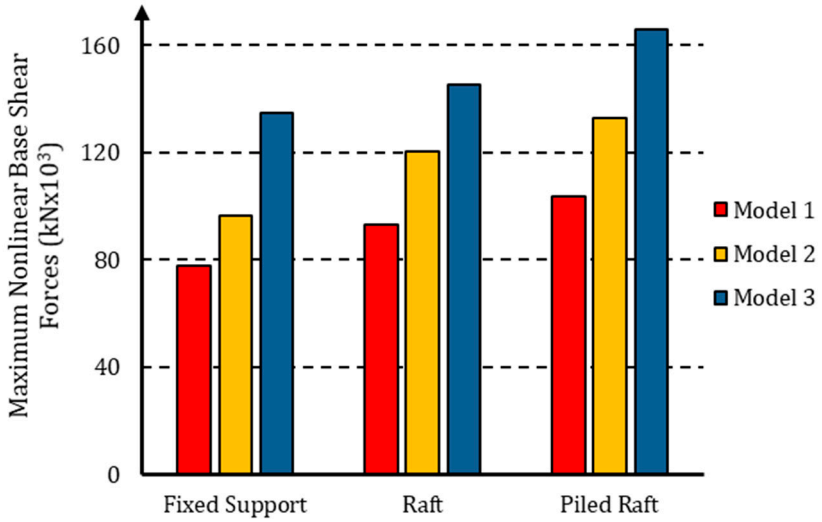


Figure 8. Comparison of absolute maximum base shear forces.

When the different SSI conditions were compared for buildings with the same structural system, the fixed-base models experienced the lowest base shear forces, while the piled raft models encountered the highest base shear forces. This circumstance can be elucidated by the allowance of the SSI condition for models to experience greater displacement, hence leading to plastic hinge formation occurring at later and lower magnitudes. The differences between the absolute maximum values of base shear forces are illustrated in Figure 8.

As can be seen in Figure 7, where the base shear forces of buildings with different structural systems with the same SSI conditions are given, the base shears acting on the buildings increased in proportion to the increase in the lateral translational stiffness of the structural system. Roof displacements resulting from these base shear forces were also compared, similar to the comparison of base shear forces. Figure 9 compares the different SSI conditions for models with the same structural system, while Figure 10 compares the roof displacement of models with different structural systems but the same SSI conditions. The differences between the absolute maximum values of roof displacement ratios are illustrated in Figure 11.

As can be seen in Figure 9, where the ratios of the roof displacements of the models with the same structural system and different SSI conditions are compared to building height, the SSI effect increases with the increase in the lateral stiffness of the structural system. This situation can be explained as follows: with the stiffening of the structural system, the rotations in the foundation increase, so the values of the additional drifts given in Figure 1 also increase. For Model 1 and Model 2, these values increased by approximately 5% from the fixed-base models to the raft foundations, and by approximately 15% from the raft foundations to the piled rafts. However, for Model 3, there was a 26% difference between the fixed-base and raft foundation and a 52% difference between the raft foundation and the piled raft. This can be explained by the fact that the structural system of Model 3 is much more rigid thanks to the 2‰ shear wall ratio. Since the lateral stiffness of the building model is very high, the high base shear already acting on the structure caused high roof displacement due to the rotations in the foundations.

The variation between the roof displacements of different structural systems under the same SSI conditions was mostly governed by the lateral stiffness of the building models. Since the foundations of rigid structural systems are more prone to rotation, the roof displacements of the analysis models other than the fixed-base model had higher values. This shows that the lateral displacement of the structures cannot be limited only by increasing the lateral stiffness of the structure and that soil effects play an important role in this regard. In fixed-base models, roof displacements increased by 17% from Model 1 to 2,

and by 10% from Model 2 to 3. Roof displacements increased by 24% from Model 1 to 2 and by 5.8% from Model 2 to 3 in the raft foundation models. Finally, in piled raft models, roof displacements increased by 23% from Model 1 to Model 2, and by 12% from Model 2 to 3.

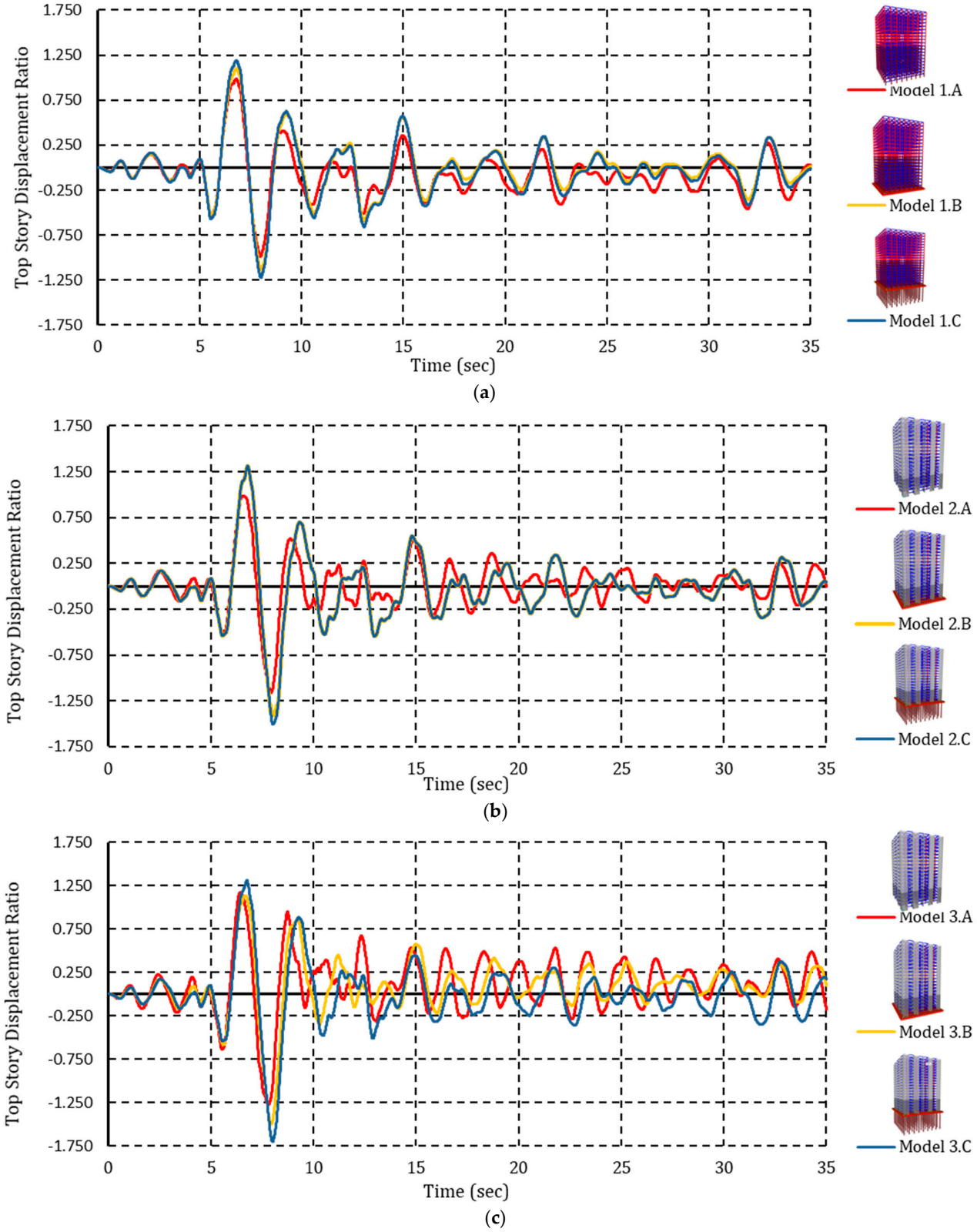


Figure 9. Top-storey displacements for models with the same structural system. (**a**) Different SSI conditions for MFs; (**b**) different SSI conditions for SW-MFs; (**c**) different SSI conditions for SWs.

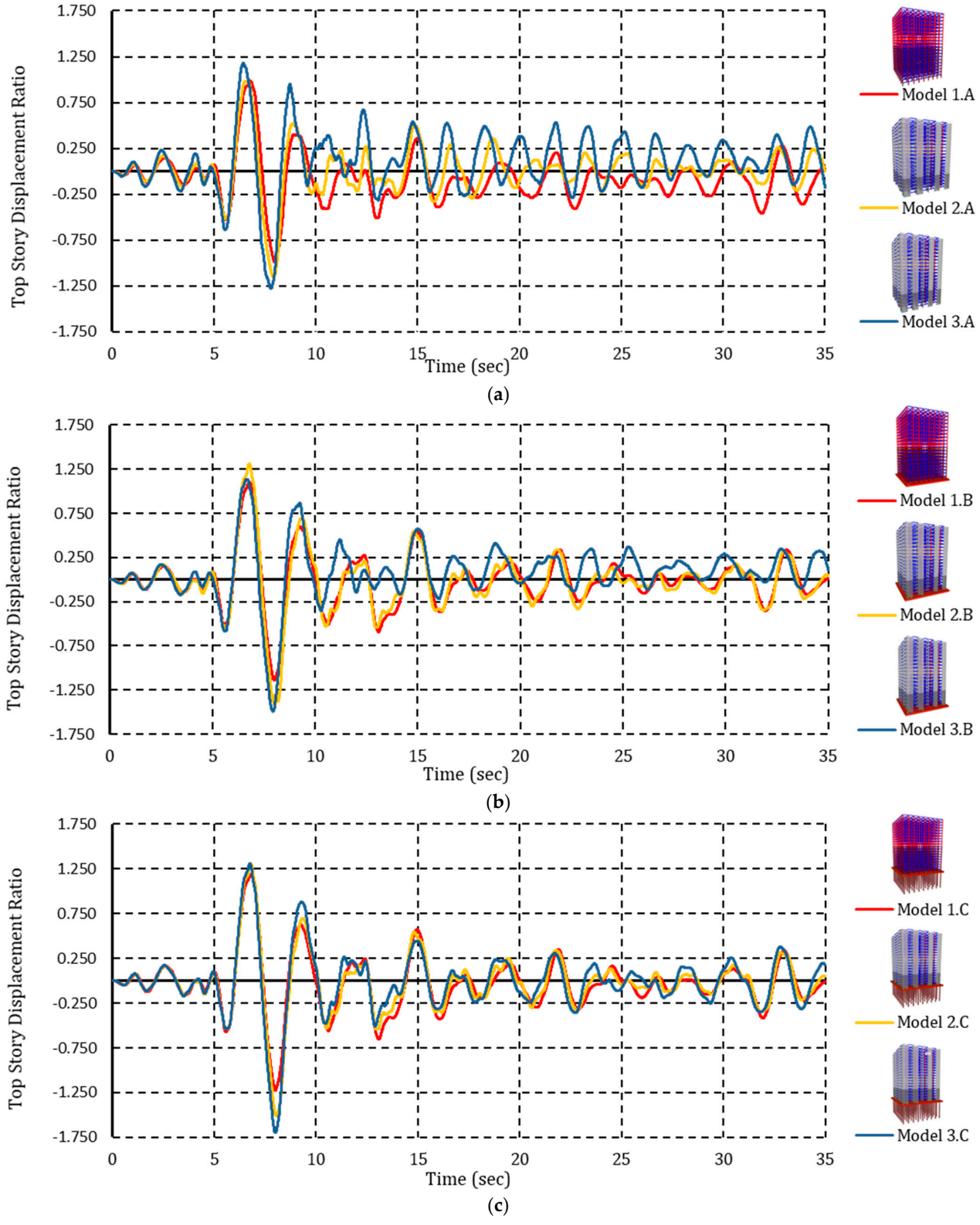


Figure 10. Top-storey displacements for models with the same SSI condition. (**a**) Different structural systems with fixed base; (**b**) different structural systems with raft foundations; (**c**) different structural systems with piled raft foundations.

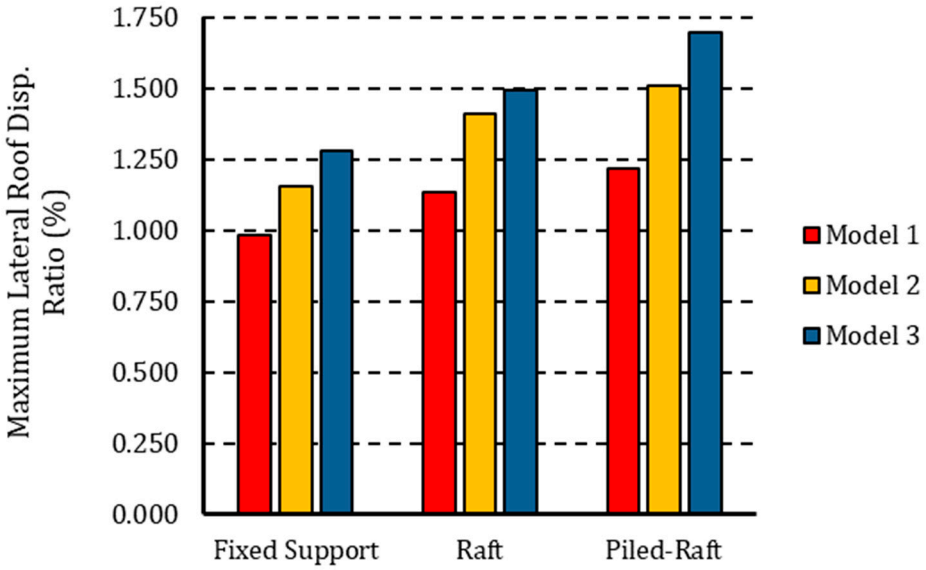


Figure 11. Comparison of absolute maximum lateral roof displacement ratios.

Considering a single-degree-of-freedom (SDOF) structure with a certain mass and lateral rigidity, if the stiffness of the structure increases, it is a predictable situation that the soil response will increase under lateral loads [56,57]. Similarly, although the structures examined in this study cannot be considered as a single-degree-of-freedom structures, they are structures with a certain lateral rigidity and mass. Therefore, stresses that vary according to this mass and rigidity occur on the soils of these structures under lateral loads.

The moment frame buildings, which had a relatively low mass, exhibited a very ductile behavior towards the moment frame buildings with RC shear walls. Rigid structures such as moment frames with RC shear walls are exposed to more lateral loads under seismic effects than moment frame buildings. In this case, the stresses and the deformations that will occur under these stresses in the soil will increase significantly as the stiffness increases.

4.2. Results for Foundations

The analyzed buildings were designed to be on soft soils, and raft foundations tend to rotate under moments caused by earthquakes. The obtained rotation values as a result of these behavioral differences are shown in Figure 12. Due to these rotations, different stress concentrations may be seen across the raft foundations. The rigidity of the superstructure plays a big role in the values and distribution of the mentioned stresses, as do the mechanical characteristics of the soil. Raft foundations are exposed to different stress distributions during an earthquake due to their rocking motions. The comparison of soil stress values for the three moments when the building models were exposed to accelerations that created critical stresses on their foundations is presented in the Appendix A. It can easily be seen in the tables given in Appendix A that the stiffness and SSI type govern the soil pressure distribution. These mentioned soil pressure values were obtained under combinations of dead, live, and time history base shear loads. It can easily be seen that the models with the piled raft foundation showed less soil pressure values than the ones with only raft foundations, thanks to the contribution of the piles. The results of the models simulated considering the SSI, as presented in Appendix A, indicate that no positive stresses occurred at any point, and hence no soil–foundation detachment was observed.

As the lateral stiffness of a building increases, the horizontal load acting on a pile element in the soil and the deformation in the direction of this load are expected to increase. The lateral force distributions and lateral displacements along the middle pile given in Figure 13 are examples of this behavior in our study.

The ability of the structures to exhibit ductile behavior allows earthquake energy to be consumed by the structural elements. But if the contribution of the soil in terms

of earthquake energy consumption is considered, the amount of energy that needs to be consumed by the building is reduced.

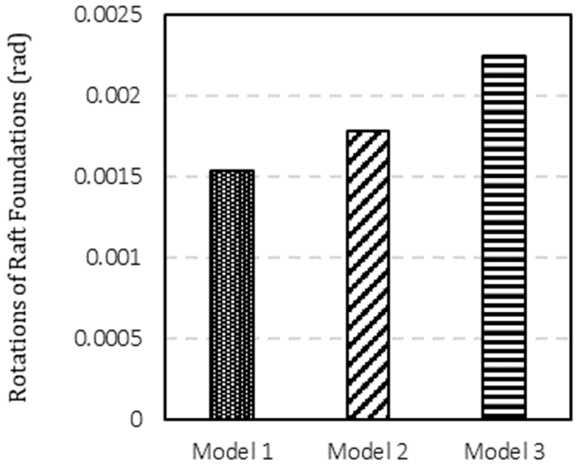
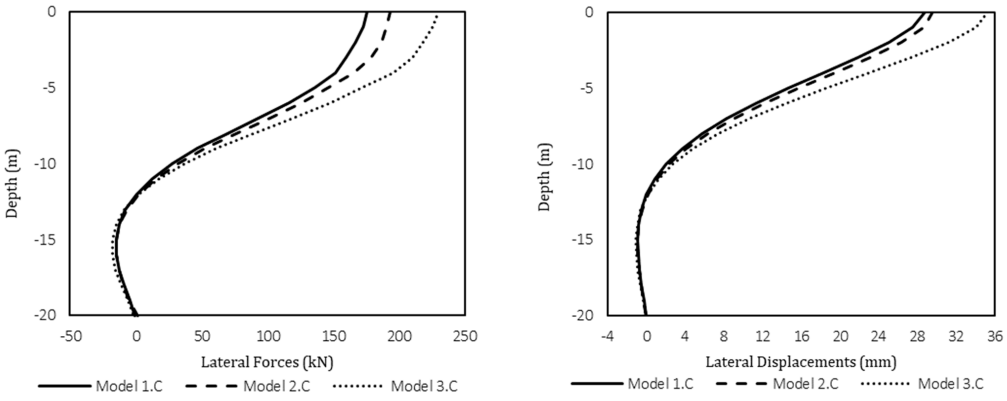


Figure 12. Rotations of raft foundations.



(**a**) (**b**)

Figure 13. (**a**) Lateral force distribution of a single pile element; (**b**) lateral displacement of a single pile element.

5. Conclusions

The results of the linear and nonlinear analyses performed on nine building models designed to investigate the effect of soil–structure interactions on the seismic behavior of 20-storey residential buildings were examined. The selection of soft soil in the SSI analysis led to high seismic demand in terms of the dynamic behavior of the soil–foundation structure system. As a result of this, the building models and soil type highlighted the inertial interaction effects. Here, compared to fixed-base models, the deformability of the SSI models created a greater amount of inter-storey and roof displacement, while at the same time highlighting the role of seismic isolation. Of course, as shown in Figure 5, the fact that the fundamental periods of the designed models were in the constant velocity region in the response spectrum was effective in reducing the base shear and inter-storey drift demands of the analysis models. The increase in the lateral stiffness of the structural systems resulted in more rigid rotations in the raft foundations. At this point, the fact that the condition defined as RC shear wall ratio in TBEC2018 [31] is the most important determinant of the response modification factors (R) used in the design phase of structural systems has become more clearly explained by the SSI analysis. This situation can of course be explained by the linear analysis results of the buildings. However, as expected, the seismic demands of the buildings decreased as the structural elements exceeded their plastic limits in the nonlinear analyses.

Due to their long fundamental periods, high-rise buildings must be capable of significant displacement. Therefore, the consideration of SSI (soil–structure interaction) should be mandatory in regulations for high-rise buildings. As the lateral stiffness of the building increases, structural displacements will decrease, but the demand for seismic force will increase, leading to greater deformations in the foundation and soil. Consequently, to prevent local and sudden soil failures during large earthquakes, buildings should be designed with deep foundations and SSI considerations.

In buildings modelled under the assumption of fixed-base conditions, a more advanced and earlier onset of plastic hinge formation was observed compared to buildings modelled with SSI in mind. The consideration of SSI relatively dampened the impact of moments on the structural system elements near the foundation, thanks to rotations in the foundation. Consequently, the levels of plastic hinge formation in the building remained at lower magnitudes, or were observed at later stages. This situation has highlighted two crucial points for consideration during the design phase. Firstly, lateral displacement values increase with the consideration of SSI. Additional checks will be required for P-Delta effects. Secondly, although buildings' lateral displacement capacities increase with the consideration of SSI, the delayed plastic hinge formation prevents structural system elements from experiencing stiffness loss, leading to an increase in the building's base shear demand (Figure 8). Thus, during SSI-informed design, both base shear and additional effects arising from P-Delta effects must be taken into account in the design of structural system elements.

The absolute maximum stresses obtained in the raft foundations reached values very close to the bearing strength of the soil at the beginning of the input record, but later on, thanks to the structural rigidity that decreased with the damage to the structural elements, they took lower values. The increase in the lateral stiffness of the structural systems resulted in higher raft-rotating demands.

Regarding the piles, increased axial forces as a result of the rocking motion did not cause plastic deformation in these elements. At the same time, looking at the analysis results, it was seen that the dynamic responses (maximum bending moments, horizontal translations) of the piles depended on the kinematic interaction.

Based on the obtained numerical results, considering the SSI in the nonlinear time history analysis of the RC building enhanced the overall structural integrity by delaying plastic hinge formation and preventing the total failure of the structural elements. Base shear forces increased by up to 20% for the same structural system under different SSI conditions, and by up to 60% for different structural systems under the same SSI conditions. Roof displacements increased by up to 17% for the same structural system under different SSI conditions, and by up to 24% for different structural systems under the same SSI conditions.

Finally, the behavioral differences required for the SSI condition, which is required only for buildings with a height of 105 m and above in TBEC2018, were also revealed for buildings with a low building importance coefficient below 105 m, which can be considered slender.

Author Contributions: Conceptualization, T.P.D. and I.H.E.; methodology, T.P.D. and I.H.E.; formal analysis, T.P.D.; investigation, T.P.D. and I.H.E.; resources, T.P.D. and I.H.E.; data curation, T.P.D.; writing—original draft preparation, T.P.D.; writing—review and editing, T.P.D.; visualization, T.P.D.; supervision, I.H.E.; project administration, I.H.E.; funding acquisition, I.H.E. All authors have read and agreed to the published version of the manuscript.

Funding: This research received no external funding.

Data Availability Statement: Most data are included in the manuscript.

Acknowledgments: This article was created from a part of Talha Polat Doğan's doctoral dissertation. Ibrahim Hakkı Erkan is the PhD Advisor of Talha Polat Doğan.

Conflicts of Interest: The authors declare no conflicts of interest.

Appendix A

Table A1. Soil pressures of MRF buildings (kPa).

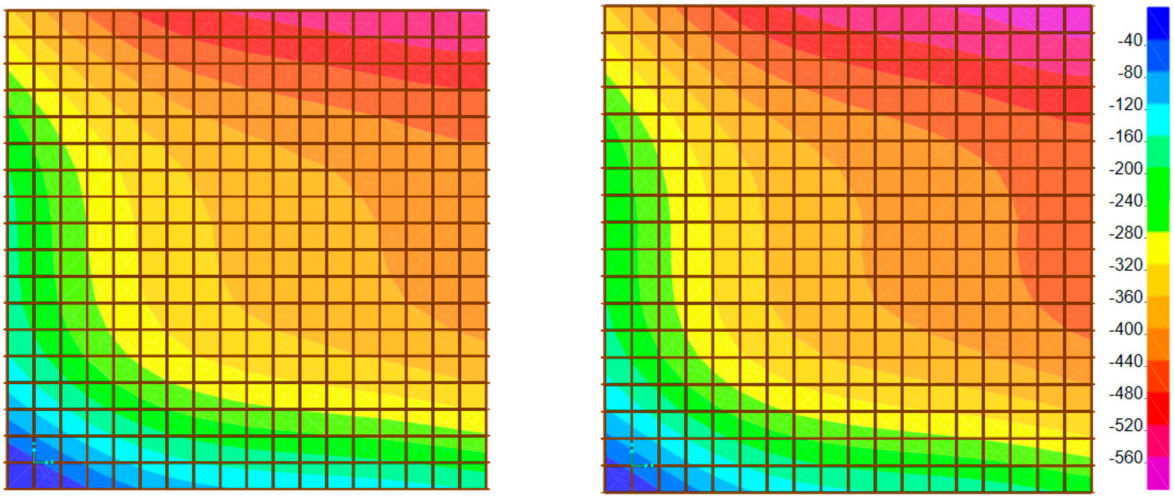
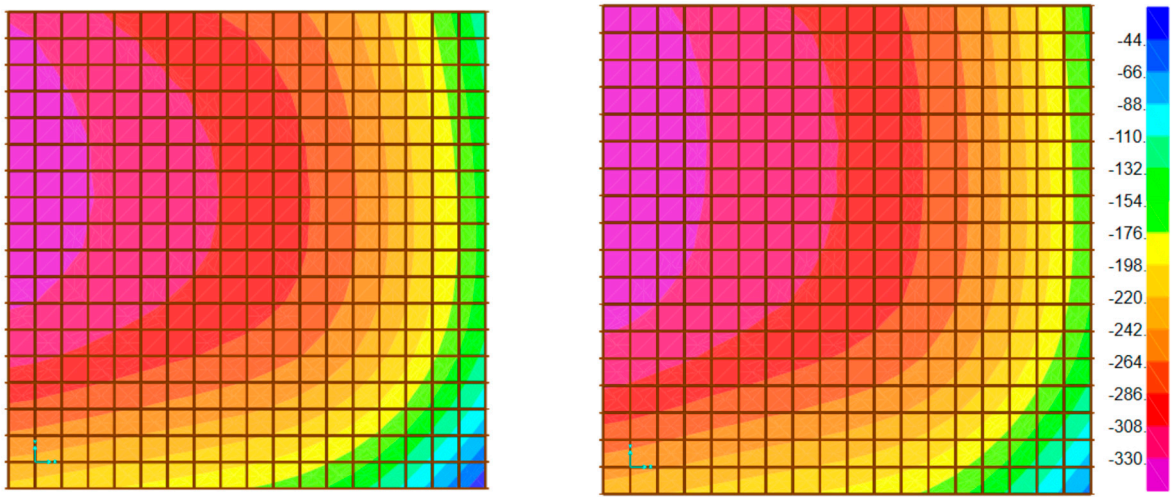
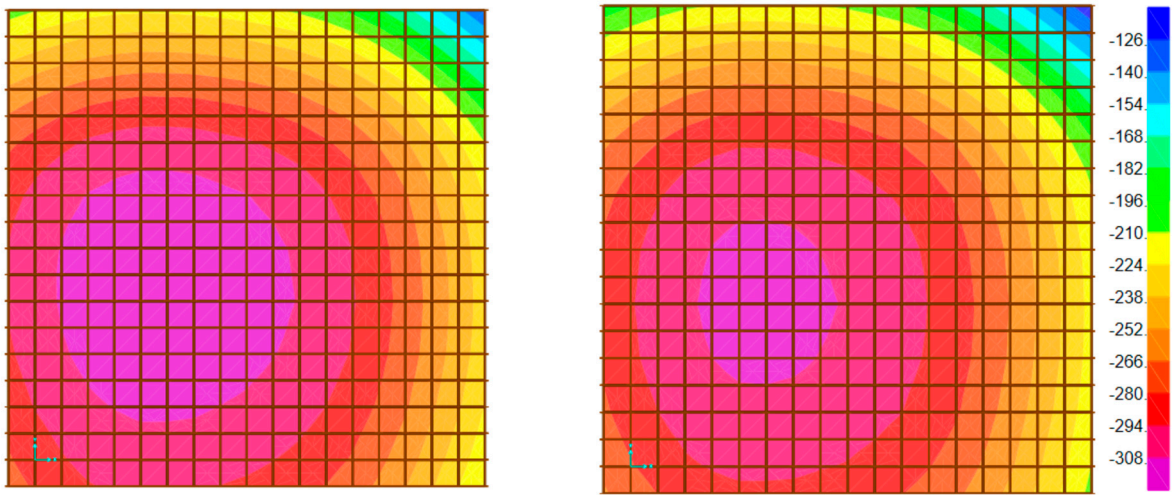
Time (s)	Structural System with MRFs	
	Raft	**Piled Raft**
7.86		
15.0		
35.0		

Table A2. Soil pressures of MRF-SWs buildings (kPa).

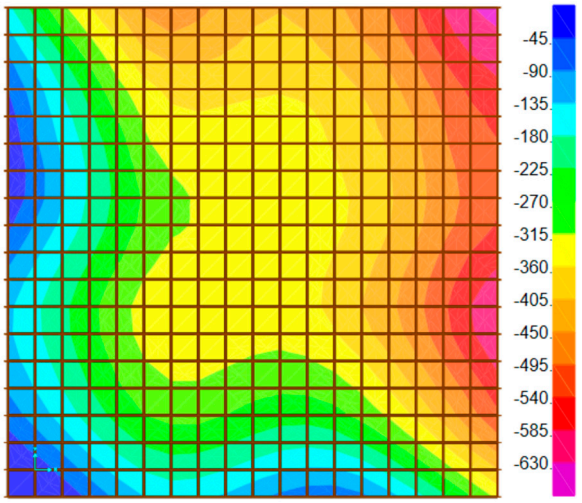
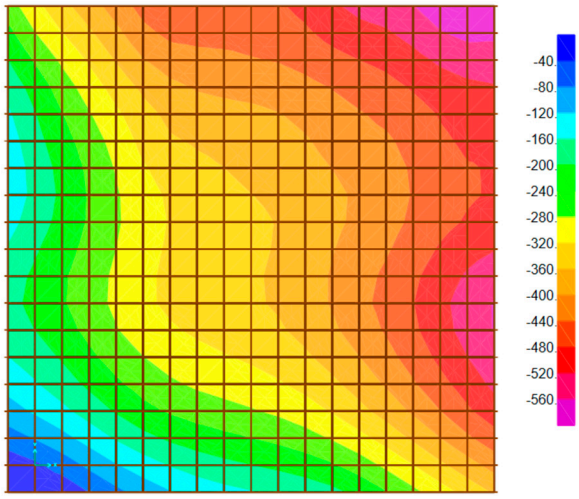
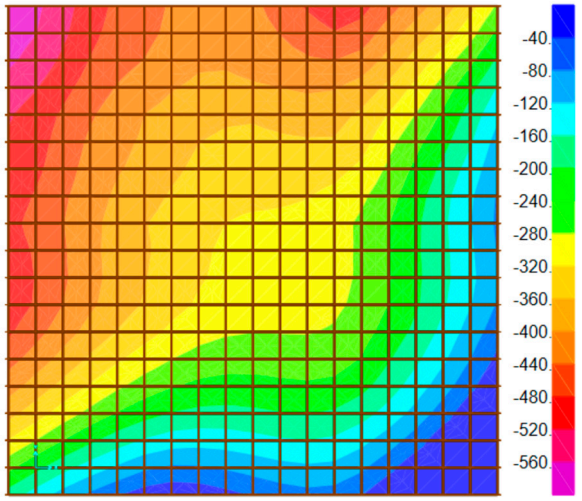
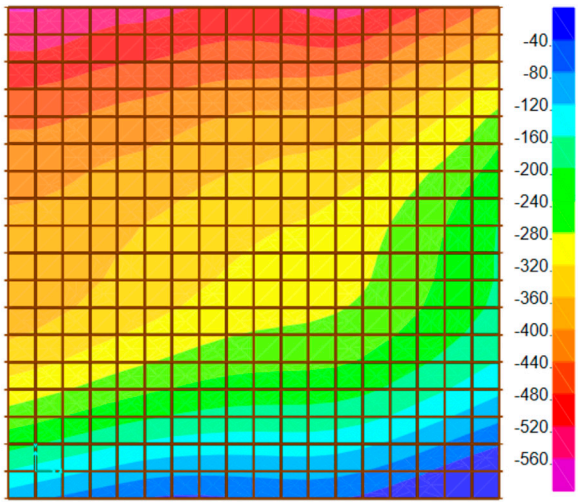
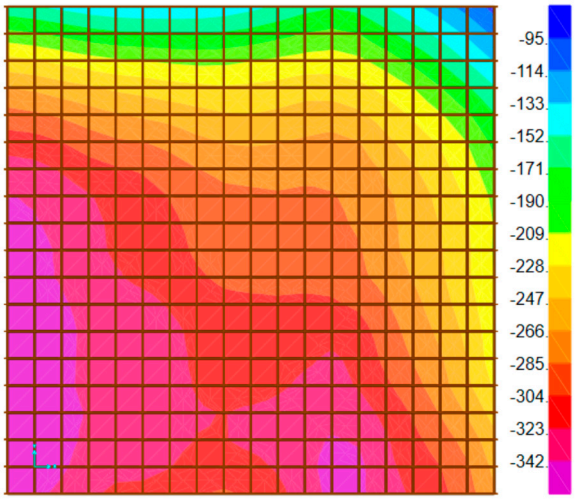
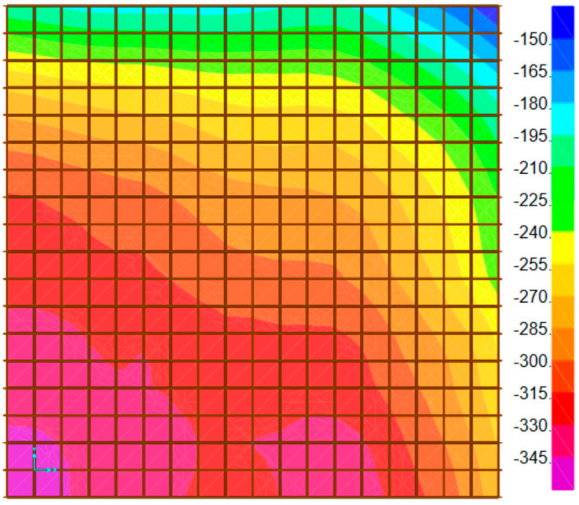
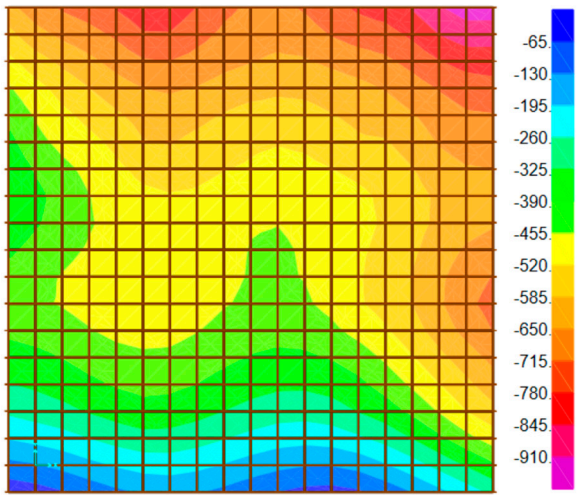
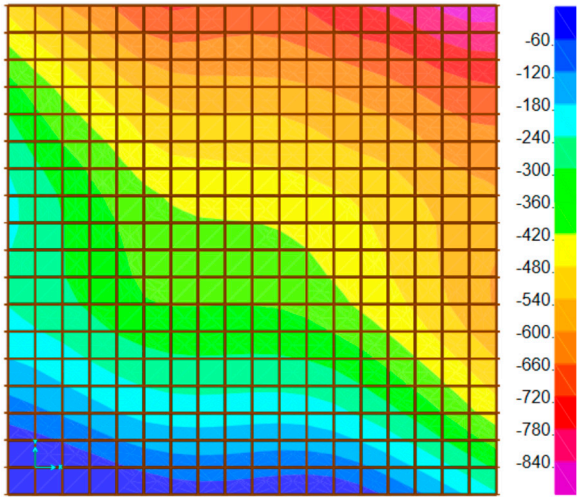
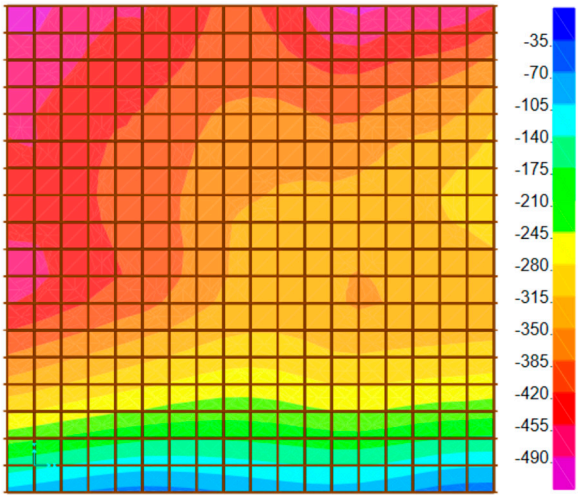
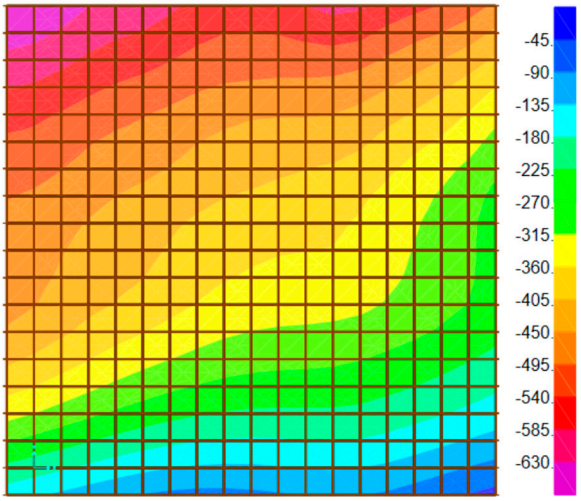
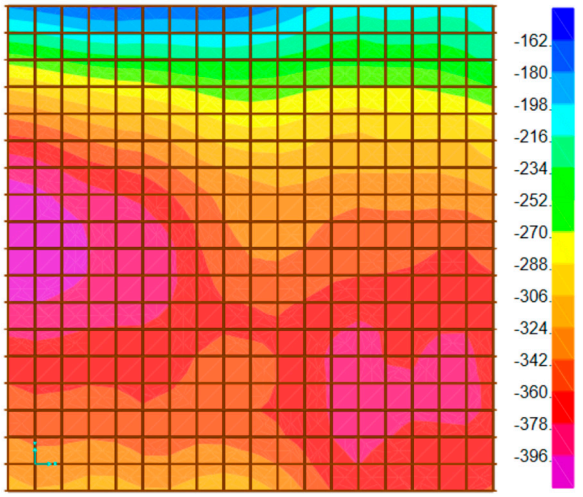
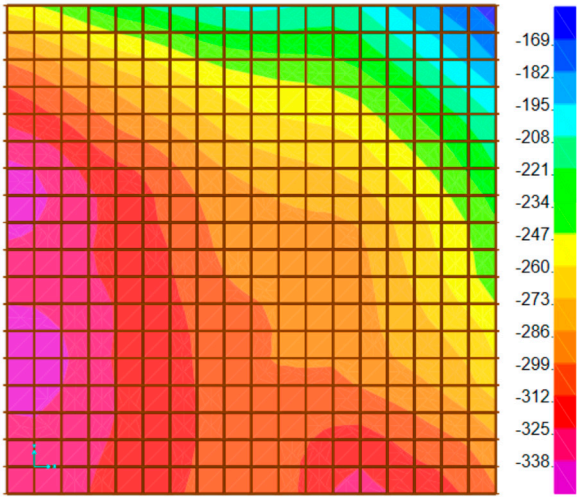
Time (s)	Structural System with MRFs and SWs	
	Raft	**Piled Raft**
7.86		
15.0		
35		

Table A3. Soil pressures of SW buildings (kPa).

Time (s)	Structural System with SWs	
	Raft	**Piled Raft**
7.86		
15.0		
35.0		

References

1. Arslan, E. P-Delta Effect in Soil-Structure Interactive Tower Structures. Master's Thesis, Kütahya Dumlupınar University, Kütahya, Turkey, 2018.
2. Garðarsson, H. Effects of Soil-Structure Interaction on the Excitation and Response of a Medium-Rise Reinforced Concrete Building. Master's Thesis, Reykjavik University, Reykjavík, Iceland, 2012.
3. Gümüş, M.; Durucan, C. Effects of pulse like ground motion records with and without acceleration pulses on the earthquake responses of structures with varying dynamic properties. *Structures* **2022**, *45*, 427–436. [CrossRef]
4. Ghorbanzadeh, M.; Khoshnoudian, F.; Taghikhany, T. A probabilistic model for the evaluation of strong column-weak beam provision for flexible-base buildings subjected to pulse-like ground motions. *Bull. Earthq. Eng.* **2022**, *20*, 997–1026. [CrossRef]
5. Hokmabadi, A.S.; Fatahi, B.; Samali, B. Assessment of soil–pile–structure interaction influencing seismic response of mid-rise buildings sitting on floating pile foundations. *Comput. Geotech.* **2014**, *55*, 172–186. [CrossRef]
6. Kechidi, S.; Colaço, A.; Costa, P.A.; Castro, J.M.; Marques, M. Modelling of soil-structure interaction in OpenSees: A practical approach for performance-based seismic design. *Structures* **2021**, *30*, 75–88. [CrossRef]
7. Tabatabaiefar, S.H.R.; Fatahi, B.; Samali, B. Numerical and experimental investigations on seismic response of building frames under influence of soil-structure interaction. *Adv. Struct. Eng.* **2014**, *17*, 109–130. [CrossRef]
8. METU-Earthquake Engineering Research Center. *Preliminary Reconnaissance Report on February 6, 2023, Pazarcık Mw=7.7 and Elbistan Mw=7.6, Kahramanmaraş-Türkiye Earthquakes*; METU-Earthquake Engineering Research Center: Ankara, Türkiye, 2023.
9. The Presidency of Strategy and Budget. *Türkiye Earthquakes Recovery and Reconstruction Assessment*; The Presidency of Strategy and Budget: Ankara, Türkiye, 2023.
10. *BS EN 1998-1:2004*; Eurocode 8: Design of Structures for Earthquake Resistance. Part 1 General Rules, Seismic Actions and Rules for Buildings. British Standards Institution: London, UK, 2005.
11. Arboleda-Monsalve, L.G.; Mercado, J.A.; Terzic, V.; Mackie, K.R. Soil–structure interaction effects on seismic performance and earthquake-induced losses in tall buildings. *J. Geotech. Geoenviron. Eng.* **2020**, *146*, 04020028. [CrossRef]
12. Qaftan, O.S.; Toma-Sabbagh, T.; Weekes, L.; Augusthus-Nelson, L. Validation of a finite element modelling approach on soil-foundation-structure interaction of a multi-storey wall-frame structure under dynamic loadings. *Soil Dyn. Earthq. Eng.* **2020**, *131*, 106041. [CrossRef]
13. Qiu, Z.; Lu, J.; Elgamal, A.; Su, L.; Wang, N.; Almutairi, A. OpenSees three-dimensional computational modeling of ground-structure systems and liquefaction scenarios. *Comput. Model. Eng. Sci.* **2019**, *120*, 629–656. [CrossRef]
14. Zhang, X.; Far, H. Effects of dynamic soil-structure interaction on seismic behaviour of high-rise buildings. *Bull. Earthq. Eng.* **2022**, *20*, 3443–3467. [CrossRef]
15. Wolf, J. *Dynamic Soil-Structure Interaction*; Prentice-Hall: Hoboken, NJ, USA, 1985.
16. Kramer, S.L. *Geotechnical Earthquake Engineering*; Pearson Education India: Chennai, India, 1996.
17. Demir, A.; Celebi, E.; Ozturk, H.; Ozcan, Z.; Ozocak, A.; Bol, E.; Sert, S.; Sahin, F.Z.; Arslan, E.; Dere Yaman, Z. Destructive impact of successive high magnitude earthquakes occurred in Türkiye's Kahramanmaraş on February 6, 2023. *Bull. Earthq. Eng.* **2024**, 1–27. [CrossRef]
18. Scarfone, R.; Morigi, M.; Conti, R. Assessment of dynamic soil-structure interaction effects for tall buildings: A 3D numerical approach. *Soil Dyn. Earthq. Eng.* **2020**, *128*, 105864. [CrossRef]
19. Savaşeri, K. The Analysis Essentials of Laterally Loaded Piles And Modelling Them With Finite Element Method. Master's Thesis, Sakarya University, Serdivan, Türkiye, 2006.
20. ur Rehman, Z.; Zhang, G. Three-dimensional elasto-plastic damage model for gravelly soil-structure interface considering the shear coupling effect. *Comput. Geotech.* **2021**, *129*, 103868. [CrossRef]
21. Mylonakis, G.; Gazetas, G. Seismic soil-structure interaction: Beneficial or detrimental? *J. Earthq. Eng.* **2000**, *4*, 277–301. [CrossRef]
22. Veletsos, A.S.; Meek, J.W. Dynamic behaviour of building-foundation systems. *Earthq. Eng. Struct. Dyn.* **1974**, *3*, 121–138. [CrossRef]
23. Mahmood, K.; ru-Rehman, Z.; Farooq, K.; Memon, S.A. One dimensional equivalent linear ground response analysis—A case study of collapsed Margalla Tower in Islamabad during 2005 Muzaffarabad Earthquake. *J. Appl. Geophys.* **2016**, *130*, 110–117. [CrossRef]
24. Mahmood, K.; Zamin, B.; Iqbal, S.; Afzal, S.; Safdar, M.; Iqbal, Q.; Ali, A. Local site effect on seismic hazard of the relocated new Balakot town. *Soil Dyn. Earthq. Eng.* **2022**, *162*, 107451. [CrossRef]
25. Pecker, A. Soil Structure Interaction. In *Advanced Earthquake Engineering Analysis*; Pecker, A., Ed.; Springer: Vienna, Austria, 2007; pp. 33–42. [CrossRef]
26. Pecker, A.; Paolucci, R.; Chatzigogos, C.; Correia, A.A.; Figini, R. The role of non-linear dynamic soil-foundation interaction on the seismic response of structures. *Bull. Earthq. Eng.* **2014**, *12*, 1157–1176. [CrossRef]
27. Barcena, A.; Esteva, L. Influence of dynamic soil–structure interaction on the nonlinear response and seismic reliability of multistorey systems. *Earthq. Eng. Struct. Dyn.* **2007**, *36*, 327–346. [CrossRef]
28. Carbonari, S.; Dezi, F.; Leoni, G. Nonlinear seismic behaviour of wall-frame dual systems accounting for soil–structure interaction. *Earthq. Eng. Struct. Dyn.* **2012**, *41*, 1651–1672. [CrossRef]
29. Zhang, J.; Tang, Y. Dimensional analysis of structures with translating and rocking foundations under near-fault ground motions. *Soil Dyn. Earthq. Eng.* **2009**, *29*, 1330–1346. [CrossRef]

30. Yünkül, K.; Gürbüz, A. Shaking table study on seismic behavior of MSE wall with inclined backfill soils reinforced by polymeric geostrips. *Geotext. Geomembr.* **2022**, *50*, 116–136. [CrossRef]
31. *TBEC2018*; Turkish Building Earthquake Code 2018. Disaster and Emergency Management Presidency: Ankara, Türkiye, 2018.
32. *Computers and Structures Incorporated Structural and Earthquake Engineering Software, C*; Sap2000 v22; Copyright Computers and Structures, Inc.: Walnut Creek, CA, USA, 2020.
33. Mander, J.B.; Priestley, M.J.; Park, R. Theoretical stress-strain model for confined concrete. *J. Struct. Eng.* **1988**, *114*, 1804–1826. [CrossRef]
34. *ASCE7-10*; American Society of Civil Engineers. Structural Engineers Assocation California: Sacramento, CA, USA, 2010; pp. 1440–1453.
35. *TS498*; Turkish Standardization Institute. Turkish Standardization Institute: Ankara, Türkiye, 1987.
36. Erkan, İ.H.; Doğan, T.P. Comparison of equivalent seismic load and response spectrum methods according to TSC 2018 and TSC 2007. *Chall. J. Struct. Mech.* **2019**, *5*, 141–153. [CrossRef]
37. *ASCE41-13*; American Society of Civil Engineers. Structural Engineers Assocation California: Sacramento, CA, USA, 2012.
38. Shahbazi, M.; Cerato, A.B.; El Naggar, M.H.; Elgamal, A. Evaluation of seismic soil–structure interaction of full-scale grouped helical piles in dense sand. *Int. J. Geomech.* **2020**, *20*, 04020228. [CrossRef]
39. Tavakoli, R.; Kamgar, R.; Rahgozar, R. Seismic performance of outrigger–belt truss system considering soil–structure interaction. *Int. J. Adv. Struct. Eng.* **2019**, *11*, 45–54. [CrossRef]
40. Tavakoli, R.; Kamgar, R.; Rahgozar, R. Optimal location of energy dissipation outrigger in high-rise building considering nonlinear soil-structure interaction effects. *Period. Polytech. Civ. Eng.* **2020**, *64*, 887–903. [CrossRef]
41. Bowles, L. *Foundation Analysis and Design*; McGraw-Hill: New York, NY, USA, 1996.
42. Winkler, E. *Theory of Elasticity and Strength*; Dominicus: Prague, Czech Republic, 1867.
43. Day, R.W. *Geotechnical Earthquake Engineering Handbook: With the 2012 International Building Code*; McGraw-Hill Education: New York, NY, USA, 2012.
44. Çelebi, E.; Göktepe, F.; Karahan, N. Non-linear finite element analysis for prediction of seismic response of buildings considering soil-structure interaction. *Nat. Hazards Earth Syst. Sci.* **2012**, *12*, 3495–3505. [CrossRef]
45. Hussien, M.N.; Karray, M.; Tobita, T.; Iai, S. Kinematic and inertial forces in pile foundations under seismic loading. *Comput. Geotech.* **2015**, *69*, 166–181. [CrossRef]
46. Lou, M.; Wang, H.; Chen, X.; Zhai, Y. Structure–soil–structure interaction: Literature review. *Soil Dyn. Earthq. Eng.* **2011**, *31*, 1724–1731. [CrossRef]
47. Amorosi, A.; Boldini, D.; Di Lernia, A. Dynamic soil-structure interaction: A three-dimensional numerical approach and its application to the Lotung case study. *Comput. Geotech.* **2017**, *90*, 34–54. [CrossRef]
48. de Silva, F.; Pitilakis, D.; Ceroni, F.; Sica, S.; Silvestri, F. Experimental and numerical dynamic identification of a historic masonry bell tower accounting for different types of interaction. *Soil Dyn. Earthq. Eng.* **2018**, *109*, 235–250. [CrossRef]
49. López Jiménez, G.A.; Dias, D.; Jenck, O. Effect of the soil–pile–structure interaction in seismic analysis: Case of liquefiable soils. *Acta Geotech.* **2019**, *14*, 1509–1525. [CrossRef]
50. Torabi, H.; Rayhani, M.T. Three dimensional finite element modeling of seismic soil–structure interaction in soft soil. *Comput. Geotech.* **2014**, *60*, 9–19. [CrossRef]
51. Terzaghi, K. Evalution of conefficients of subgrade reaction. *Geotechnique* **1955**, *5*, 297–326. [CrossRef]
52. Gazetas, G. Formulas and charts for impedances of surface and embedded foundations. *J. Geotech. Eng.* **1991**, *117*, 1363–1381. [CrossRef]
53. DEMP. Seismic Hazard Maps Interactive Web Application. Disaster and Emergency Management Presidency: Ankara, Türkiye, 2018. Available online: https://tdth.afad.gov.tr/ (accessed on 14 January 2024).
54. Databases, P.S.G. Pasific Earthquake Engineering Research Center. *Berkeley University*. 2000. Available online: https://peer.berkeley.edu/peer-strong-ground-motion-databases (accessed on 14 January 2024).
55. Soyluk, K.; Sicacik, E.A. Soil–structure interaction analysis of cable-stayed bridges for spatially varying ground motion components. *Soil Dyn. Earthq. Eng.* **2012**, *35*, 80–90. [CrossRef]
56. Gazetas, G.; Psarropoulos, P.; Anastasopoulos, I.; Gerolymos, N. Seismic behaviour of flexible retaining systems subjected to short-duration moderately strong excitation. *Soil Dyn. Earthq. Eng.* **2004**, *24*, 537–550. [CrossRef]
57. Veletsos, A.S.; Younan, A.H. Dynamic modeling and response of soil-wall systems. *J. Geotech. Eng.* **1994**, *120*, 2155–2179. [CrossRef]

Disclaimer/Publisher's Note: The statements, opinions and data contained in all publications are solely those of the individual author(s) and contributor(s) and not of MDPI and/or the editor(s). MDPI and/or the editor(s) disclaim responsibility for any injury to people or property resulting from any ideas, methods, instructions or products referred to in the content.